

## Modeling of electronic transport in scanning tunneling microscope tip–carbon nanotube systems

Toshishige Yamada<sup>a)</sup>

NASA Ames Research Center, M/S T27A-1, Moffett Field, California 94035-1000

(Received 22 September 2000; accepted for publication 26 January 2001)

A model is proposed for two observed current–voltage ( $I$ – $V$ ) patterns in a recent experiment with a scanning tunneling microscope tip and a carbon nanotube [Collins *et al.*, *Science* **278**, 100 (1997)]. We claim that there are two mechanical contact modes for a tip (metal)–nanotube (semiconductor) junction (1) with or (2) without a tiny vacuum gap (0.1–0.2 nm). With the tip grounded, the tunneling case in (1) would produce large  $dI/dV$  with  $V>0$ , small  $dI/dV$  with  $V<0$ , and  $I=0$  near  $V=0$  for an either  $n$  or  $p$  nanotube; the Schottky mechanism in (2) would result in  $I\neq 0$  only with  $V<0$  for an  $n$  nanotube, and the bias polarities would be reversed for a  $p$  nanotube. The two observed  $I$ – $V$  patterns are thus entirely explained by a tip–nanotube contact of the two types, where the nanotube must be  $n$ -type. © 2001 American Institute of Physics. [DOI: 10.1063/1.1357206]

Current–voltage ( $I$ – $V$ ) characteristics have been reported by Collins *et al.* for a system with a scanning tunneling microscope (STM) tip and a carbon nanotube at room temperature.<sup>1</sup> The STM tip was driven forward into a film of many entangled nanotubes on a substrate, and then was retracted well beyond the normal tunneling range. At a distance of  $\sim 0.1$   $\mu\text{m}$  above the surface, there was usually electronic conduction between the tip and the film since nanotubes bridged the two regions. At  $\sim 1$   $\mu\text{m}$ , only one nanotube remained occasionally, and the electronic conduction was still maintained. One end of the nanotube continued sticking to the tip during retraction, while the other consistently stayed in the film.  $I$ – $V$  characteristics for this tip–nanotube system had two different patterns for low ( $<1.95$   $\mu\text{m}$ ) and high (1.98  $\mu\text{m}$ ) tip-to-film distances as schematically shown in Figs. 1(a) and 1(b). The lower-distance cases showed large  $dI/dV$  with  $V>0$ , small  $dI/dV$  with  $V<0$ , and  $I=0$  near  $V=0$  (type I), while the high-distance case showed rectification, i.e.,  $I\neq 0$  only with  $V<0$  (type II), if the tip was grounded (different bias definition from that in Ref. 1). In this letter we propose a physical mechanism to explain the observed  $I$ – $V$  patterns.

We consider that the observed characteristics strongly reflected the nature of the tip (metal)–nanotube (semiconductor) contact. The other end of the nanotube was entangled well into the film, and simply provided good ohmic contact. We will argue that there are two different mechanical contact modes, vacuum gap (left) and touching (right) modes as in Fig. 1(c), depending on the presence or absence of a tiny vacuum gap  $d\sim 0.1$ – $0.2$  nm at the junction. These modes are analogous to physisorption and chemisorption, respectively. Once admitting their existence, it is naturally shown that  $I$ – $V$  characteristics are type I in the vacuum gap mode and type II in the touching mode. We will show that the nanotube had to be an  $n$ -type semiconductor, unlike often observed

$p$ -type semiconducting nanotubes<sup>2</sup> in field-effect-transistor (FET) applications.<sup>3</sup>

Experimentally, the STM tip was not placed at the end of the nanotube as if it were an extension, but contacted the side of the nanotube so that the tip and nanotube surfaces faced each other. Thus, one-dimensional cylindrical junction effects<sup>4</sup> are not relevant here. Additionally, in Ref. 5 it was shown that nanotubes will generally flatten on a substrate due to van der Waals interaction. A nanotube will flatten at the STM tip surface in both contact modes shown in Fig. 1. Therefore, the tip–nanotube junction is approximated well by the traditional planar junction model.<sup>3</sup>

Band diagrams are shown in Figs. 1(d)–1(f) for type I (left) and in Figs. 1(g)–1(i) for type II (right). On the metal side,  $E_{FM}$  is the Fermi energy and  $\phi_M$  is the work function. On the semiconductor side,  $\chi$  is the electron affinity,  $E_{FS}$  is the Fermi energy, and  $E_G$  is the band gap.  $E_c$  and  $E_v$  are conduction and valence band edges, respectively, and depend on the applied voltage  $V$  after the tip is grounded.  $\phi_n$  and  $\phi_p$  are Schottky barriers and  $\xi = E_{FS} - E_v$ . In Fig. 1(d), valence-band electrons tunnel to the tip with  $V<0$ , resulting in smaller  $dI/dV$ . Figure 1(e) shows a thermal equilibrium with  $V=0$ . In Fig. 1(f), tip electrons tunnel to the conduction band with  $V>0$ , resulting in larger  $dI/dV$ . The vacuum gap provides flexibility for  $E_c$  and  $E_v$  to align freely with  $E_{FM}$  by absorbing the necessary voltage drop for a given  $V$ . In the touching mode,  $\phi_n$  and  $\phi_p$  are fixed regardless of  $V$ . The Schottky forward transport occurred at the same bias polarity as the valence-band tunneling of Fig. 1(d) did. Thus, Fig. 1(g) follows with  $V<0$ , and the nanotube has to be  $n$  type. Figure 1(h) shows thermal equilibrium and Fig. 1(i) shows a reverse condition with  $V>0$  with negligible current. We note that for  $p$  nanotubes, the entire  $I$ – $V$  pattern simply shifts to the positive  $V$  direction in the vacuum gap mode, while it rotates  $180^\circ$  in the touching mode. Thus, if the Schottky forward transport had occurred at the same polarity as the conduction-band tunneling of Fig. 1(f) ( $V>0$ ), then the nanotube would have been  $p$  type.

In the vacuum gap mode, we assume that the total en-

<sup>a)</sup>Also at: CSC; electronic mail: yamada@nas.nasa.gov

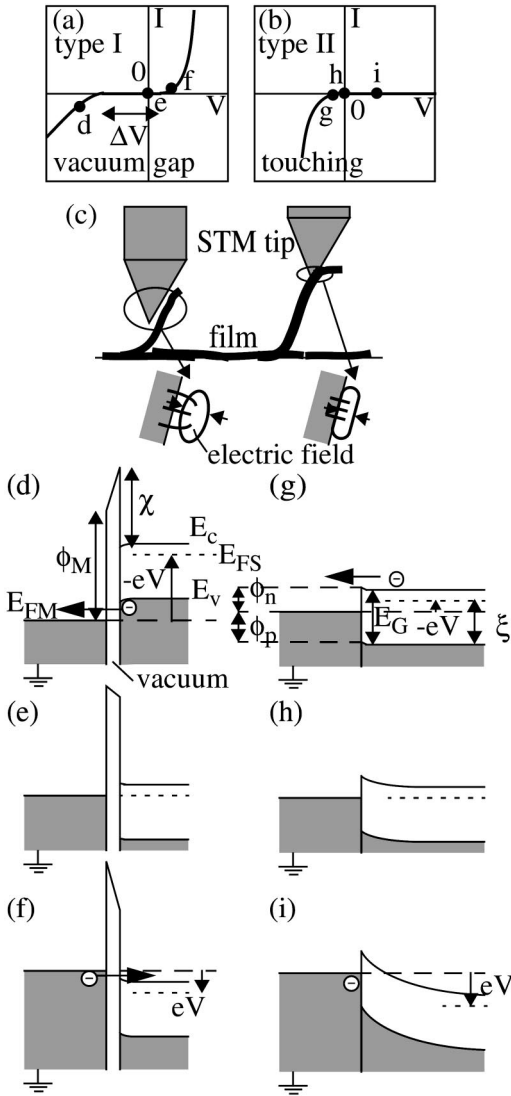


FIG. 1. STM tip–nanotube system with two mechanical contact modes: (a) type-I and (b) type-II  $I$ – $V$  patterns. (c) Schematic showing the vacuum gap (left) and touching (right) modes. (d)–(i) Band structures for operation points in the  $I$ – $V$  patterns: (d) valence-band tunneling ( $V < 0$ ), (e) equilibrium ( $V = 0$ ), (f) conduction-band tunneling ( $V > 0$ ), (g) Schottky forward ( $V < 0$ ), (h) equilibrium ( $V = 0$ ), and (i) Schottky reverse ( $V > 0$ ), where the STM tip is grounded.

ergy  $E$  and the parallel momentum  $k_\rho = (k_x^2 + k_y^2)^{1/2}$  are conserved in the tunneling,<sup>6</sup> where  $k_x$  and  $k_y$  are transverse and longitudinal momenta, respectively. Nanotubes are finite in the  $x$  direction, and  $k_x$  is not exactly conserved, while  $k_y$  is.<sup>7</sup> Both are conserved for infinitely wide nanotubes. The nanotube used in the experiment is sufficiently wide that the subbands are treated as a group in a  $k_\rho$  integration with the effective mass  $m_i$  for band  $i$  ( $i = c, v$ ). We consider a *semi-conducting* (17, 0) nanotube with a 1.33 nm diameter, the closest to the experimental 1.36 nm (Ref. 1) in the zigzag tube families.<sup>8</sup> Valence and conduction subbands are given in Ref. 8 by  $E_v(k, n) = -f(k, n)$  and  $E_c(k, n) = f(k, n)$  ( $n = 1, 2, \dots, 17$ ), respectively, where  $f(k, n) = |V_{pp\pi}| [1 \pm 4 \cos(\sqrt{3}ka/2) \cos(n\pi/17) + 4 \cos^2(n\pi/17)]^{1/2}$ .  $V_{pp\pi}$  is an overlap integral ( $-2.5$  eV),  $a$  is a lattice period (0.246 nm), and  $k$  is the momentum along the tube ( $-\pi/\sqrt{3}a < k < \pi/\sqrt{3}a$ ). There are 34 valence subbands and 34 conduction subbands. We evaluate  $m_i$  by averaging the inverse

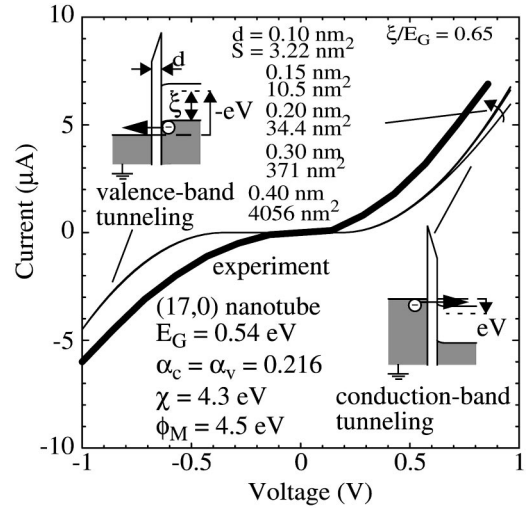


FIG. 2. Type-I  $I$ – $V$  characteristics (with experimental data of Ref. 1), calculated with the tunneling formula in the vacuum gap mode.

masses of the first 17 subbands from the band gap for each band (i.e., valence subbands with a top at  $\Gamma$ , or conduction subbands with a bottom at  $\Gamma$ ), respectively, and find  $m_c/m(= \alpha_c) = m_v/m(= \alpha_v) = 0.216$  with  $m$  being the vacuum electron mass. The tunneling current  $I_i$  via band  $i$  at zero temperature is given (the upper sign for  $c$  and the lower for  $v$ ) by<sup>6,9</sup>

$$I_i = \frac{4\pi m e S}{h^3} \int_{E_{FM} - eV}^{E_{FM}} dE \theta[\pm \{E - E_i(V)\}] \times \int_{E(1 \mp \alpha_i) \pm \alpha_i E_i(V)}^E dW D(W), \quad (1)$$

where the integrations are performed for  $E$  and normal ( $z$ ) energy  $W$  (converted from the  $k_\rho$  integration) in the metal. The lower limit of  $W$  integration is complicated due to the  $E - k_\rho$  conservation discussed above.  $e$  is the unit charge,  $S$  is the tip–nanotube overlap area,  $h$  is the Planck constant, and  $\theta$  is a step function.  $D$  is a transmission coefficient and assumed to depend only on  $W$ .<sup>9</sup>  $E_G = 0.54$  eV and  $\chi = 4.6$  eV (graphite work function)  $-E_G/2 = 4.3$  eV for a (17,0) nanotube,<sup>8,10</sup> and  $\phi_M = 4.5$  eV for a tungsten tip. These numbers define the vacuum barrier height, and  $D(W)$  is calculated with a Wentzel–Kramers–Brillouin (WKB) approximation.<sup>6</sup> Image potential<sup>3,6</sup> is not considered, and the semiconductor band bending<sup>3,9</sup> is neglected, but they do not change our qualitative conclusions.  $S$ ,  $d$ , and  $\xi$  will be determined to fit the experimental  $I$ – $V$  data best.

In Fig. 2 the vacuum gap mode leading to the type-I  $I$ – $V$  characteristics is assumed.  $\xi$  shifts the entire  $I$ – $V$  curve horizontally and the best fit is obtained for  $\xi/E_G = 0.65 (> 0.5)$ . This is consistent with our conclusion that the nanotube was  $n$  type. For very large  $d$  such as 0.40 nm,  $dI/dV$  asymmetry for opposite polarities is more enhanced than in the experiment, and  $S$  is unreasonably large  $\sim 4000$  nm<sup>2</sup>. This is certainly not the case. For  $d \sim 0.1 - 0.2$  nm with  $S \sim 3 - 34$  nm<sup>2</sup>, the curves are indistinguishable.  $d$  is measured from the natural separation defined by the surface bonding, and there is no lower limit.  $S$  should be around  $10^{0-1}$  nm<sup>2</sup>. Thus, these are all likely candidates, and we will not narrow it down further. The calculated current is smaller than the measured

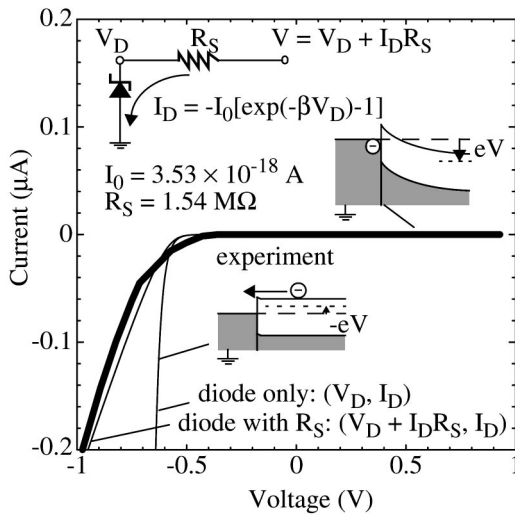


FIG. 3. Type-II  $I$ - $V$  characteristics (with experimental data of Ref. 1), calculated with the Schottky formula in the touching mode.

one and the measured voltage interval  $\Delta V$  for  $I=0$  seems narrower than  $E_G/e=0.54$  V.  $E_G$  greatly depends on the diameter, and large deviation from the above value is unlikely (e.g.,  $E_G=0.4$  eV for a diameter as large as 1.8 nm).<sup>11</sup> The semiconductor band bending and the finite temperature (the experiment was carried out at room temperature) reduce  $\Delta V$  effectively,<sup>9</sup> and they would explain the discrepancy. We do not explicitly include a series resistance  $R_S$  representing the bulk film resistance and the film-electrode contact resistance, etc.  $R_S$  is implicitly included in  $d$  and  $S$ . The overall fitting is reasonable, and the results correctly recover large  $dI/dV$  with  $V>0$  and small  $dI/dV$  with  $V<0$ , one of the key experimental findings.<sup>1</sup>

In Fig. 3 the touching mode leading to the type-II  $I$ - $V$  characteristics is assumed. We explicitly include  $R_S$  this time. In an equivalent circuit with a Schottky diode and  $R_S$ , the diode current  $I_D$ , the diode voltage  $V_D$ , and the total voltage  $V$  are related by  $I_D = -I_0[\exp(-\beta V_D) - 1]$  and  $V = V_D + I_D R_S$  with  $\beta$  the inverse temperature.  $I_0$  is a constant related to  $S$  and  $\phi_n$ . The diode-only characteristics ( $V_D, I_D$ ) are plotted in Fig. 3 with  $I_0 = 3.53 \times 10^{-18}$  A, resulting in a discrepancy. We thus introduce  $R_S = 1.54$  M $\Omega$ , and plot the characteristics ( $V_D + I_D R_S, I_D$ ). This recovers the experiment well.

The experimental current level in Fig. 3 is smaller than that in Fig. 2. In the former, the tip-nanotube binding will be weak (physisorption like) and there will be a vacuum gap, so that  $S$  will be too large in order to support the tension on the nanotube from the film. In the latter, the tip-nanotube binding will be stronger and  $S$  can be smaller. This is because the tension always tends to reduce  $S$  by pulling the nanotube down.  $S$  will be minimized in the touching mode where the binding is strongest (chemisorption like). In fact, we can recover the above  $I_0 \sim 3 \times 10^{-18}$  A by expecting, e.g.,  $S \sim 0.1$  nm<sup>2</sup> and  $\phi_n \sim 0.5$  eV ( $< E_G$ ) with the Richardson constant  $A^* \sim 10^1$  A/cm<sup>2</sup>/K<sup>2</sup> in  $I_0 = SA^* T^2 \exp(-\beta \phi_n)$ ,<sup>3</sup> where  $T$  is the temperature.  $S$  and  $\phi_n$  in these ranges are possible. For further investigation,  $S$ ,  $\phi_n$ , and  $A^*$  need to be determined experimentally.

Similar  $I$ - $V$  characteristics to the type I here have also been observed for drain current versus drain voltage in nanotube FETs.<sup>2</sup> However, some results were not due to the scenario discussed here, but due to the Coulomb blockade mechanism<sup>12</sup> for shorter nanotubes ( $\sim 0.1$   $\mu$ m) at much lower temperatures ( $\sim 4.2$  K). Such an example was reported in Ref. 13. We have shown that the nanotube was  $n$  type.<sup>14</sup> It was freshly out of the film and was hanging in air throughout the experiment.<sup>1</sup> On the other hand, nanotubes placed on a silicon dioxide surface in the FET applications were consistently  $p$  type regardless of their lengths (0.3–3  $\mu$ m).<sup>2</sup> Contact electrodes probably could not provide holes everywhere in long nanotubes. The observed  $p$ -type behavior would be related to the trapped charges<sup>3</sup> in the silicon dioxide layer of the FET structure, and/or oxidation.<sup>14</sup>

In summary, the observed experimental  $I$ - $V$  characteristics<sup>1</sup> for the STM tip-nanotube system are explained with a tip-nanotube contact model. In the vacuum gap mode, we expect different  $dI/dV$  at opposite bias polarities and  $I=0$  near  $V=0$  reflecting the conduction- and valence-band tunneling. In the touching mode, the  $I$ - $V$  characteristics are rectifying, because of the usual Schottky mechanism. We have argued that the Schottky forward transport occurred at the same bias polarity as the valence-band tunneling did in the experiment, and concluded that the nanotube was an  $n$ -type semiconductor.

The author acknowledges M. Meyyappan, T. R. Govindan, R. A. Kiehl (University of Minnesota), and B. A. Biegel for fruitful discussions.

<sup>1</sup> P. G. Collins, A. Zettl, H. Bando, A. Thess, and R. E. Smalley, *Science* **278**, 100 (1997).

<sup>2</sup> S. J. Tans, A. R. M. Verschueren, and C. Dekker, *Nature (London)* **393**, 49 (1998); R. Martel, T. Schmidt, H. R. Shea, T. Hertel, and Ph. Avouris, *Appl. Phys. Lett.* **73**, 2447 (1998); T. Yamada, *ibid.* **76**, 628 (2000); C. Zhou, J. Kong, and H. Dai, *ibid.* **76**, 1597 (2000).

<sup>3</sup> S. M. Sze, *Physics of Semiconductor Devices*, 2nd ed. (Wiley, New York, 1981).

<sup>4</sup> F. Leonard and J. Tersoff, *Phys. Rev. Lett.* **83**, 5174 (1999).

<sup>5</sup> T. Hertel, R. E. Walkup, and Ph. Avouris, *Phys. Rev. B* **58**, 13870 (1998).

<sup>6</sup> C. Duke, *Tunneling in Solids*, Solid State Physics, Suppl. 10, edited by F. Seitz and D. Turnbull (Academic, New York, 1969); J. Bono and R. H. Good, Jr., *Surf. Sci.* **175**, 415 (1986).

<sup>7</sup> P. Delaney and M. Di Ventra, *Appl. Phys. Lett.* **75**, 4028 (1999).

<sup>8</sup> R. Saito, M. Fujita, G. Dresselhouse, and M. S. Dresselhouse, *Phys. Rev. B* **46**, 1804 (1992); M. S. Dresselhaus, G. Dresselhouse, and P. C. Eklund, *Science of Fullerenes and Carbon Nanotubes* (Academic, San Diego, 1996).

<sup>9</sup> R. M. Feenstra and J. A. Stroscio, *J. Vac. Sci. Technol. B* **5**, 923 (1987).

<sup>10</sup> According to the tight-binding picture, the band gap opens symmetrically when a graphite sheet is rolled up to form a semiconducting nanotube, and therefore, the graphite work function corresponds to the middle of the gap.

<sup>11</sup> J. W. Mintimore and C. T. White, *Carbon* **33**, 893 (1995); the diameter of 1.3 nm was directly measured with a STM in L. C. Venema, J. W. G. Wildöer, J. W. Janssen, S. J. Tans, H. L. J. Temminic Tuinstra, L. P. Kouwenhoven, and C. Dekker, *Science* **283**, 52 (1999).

<sup>12</sup> D. V. Averin and K. K. Likharev, *J. Low Temp. Phys.* **62**, 345 (1986); A. Bezryadin, A. R. M. Verschueren, S. J. Tans, and C. Dekker, *Phys. Rev. Lett.* **80**, 4036 (1998).

<sup>13</sup> H. R. Shea, R. Martel, T. Hertel, T. Schmidt, and Ph. Avouris, *Microelectron. Eng.* **46**, 101 (1999).

<sup>14</sup> G. U. Sumanasekera, C. K. W. Adu, S. Fang, and P. C. Eklund, *Phys. Rev. Lett.* **85**, 1096 (2000).